Some aspects of the role of intergranular fluids in the compositional evolution of metamorphic rocks

Sumit Chakraborty and Ralf Dohmen

Institut für Geologie, Mineralogie und Geophysik, Ruhr-Universität Bochum, D-44780 Bochum, Germany.

Minerals that react with each other during the progressive evolution of metamorphic terranes are not always in physical contact. As such, an "intergranular fluid" could play a major role in element transfer and chemical evolution. However, the nature of this fluid and its specific role remains somewhat elusive. Recent experiments in our laboratory shed some light on the behavior of such a fluid. Here we present a simple mathematical model which accounts for diffusion within crystals and fluid, solubility in the fluid and mass balance between the various reservoirs. The model elucidates the nature of element exchange between two minerals via the mediation of an intergranular fluid. It is shown that a coupling of thermodynamics and kinetics controls the evolution of the system and the concentration of an element in the intergranular fluid is a key parameter of interest.

The results have important implications for standard tools of metamorphic petrology such as geothermometers and barometers, geospeedometry and the closure of isotopic systems. For example, homogeneity of mineral grains may be a poor criterion for equilibrium and the rim compositions of minerals showing diffusion zoning may be out of equilibrium with distant exchange partners, even in the presence of a fluid in which transport is fast.

1. Introduction

The last century saw a major shift in emphasis in the study of metamorphic rocks—from a descriptive science attempting to use qualitative and graphical tools to unravel the history of these rocks to a field where principles of equilibrium thermodynamics, and to some extent kinetics, were employed to glean a quantitative understanding. As these applications have reached a certain level of maturity, they have brought forth the need for a deeper understanding of metamorphic processes. Thus, the start of a new century coincides with yet another shift in focus of the metamorphic petrologist—from the rocks themselves to the processes that formed them, from a quantitative documentation of the conditions of formation to tracing the events that lead to solid state transformations in nature, the ultimate product of which we call a metamorphic rock. Tracing the processes requires a deeper understanding of the mechanisms by which such transformations occur. In turn, an understanding of the processes by which metamorphic reactions occur reveal potential shortcomings of many assumptions underlying the formulation of routinely used tools such as geothermometers, geobarometers and geospeedometers. This enables the petrologist to make more refined use of these tools, with an awareness of their pitfalls and limitations.

One concept that is deeply embedded in the tradition of metamorphic petrology is that of the hypothetical "intergranular fluid". While its existence has been implied in many analyses of metamorphic textures since the beginning of the discipline, actual quantitative reference to the fluid and its properties began to be made in the sixties and early seventies as thermodynamics and kinetics began to play an increasingly prominent role, the thermodynamic context being derived directly

Keywords. Intergranular fluid; metamorphism; diffusion; geothermometry; closure temperature.

Proc. Indian Acad. Sci. (Earth Planet. Sci.), **110**, No. 4, December 2001, pp. 293–303

from the works of J W Gibbs. However, while transport and equilibrium properties were attributed to the intergranular fluid, its specific nature and identity remained largely elusive. Recent experiments which make an unconventional use of Knudsen-cell mass spectrometry provide us with some insight into this problem. In this work we combine the results obtained from some of these experiments with theoretical modelling to address the question: How does element partitioning (e.g. geothermometers) progress in nature? We begin by summarizing our experimental setup and some of the relevant observations, which have been published elsewhere (Dohmen *et al* 1998, 2001). The next section presents a simple model to simulate element partitioning between two crystals which are physically separated and communicate with each other via an "intergranular fluid". The results bring forth a series of surprises which challenge some of the basic tenets of geothermometry and petrologic phase equilibria in general. For example, homogeneity of reacting crystals is no guarantee of equilibrium, and the rim compositions of zoned crystals may have little to do with equilibrium partitioning!

1.1 *The experiments – Knudsen-cell mass spectrometry*

A Knudsen cell consists of a device which has a hole small enough in dimension such that gases can effuse through it as a molecular beam (i.e. Knudsen diffusion; Knudsen 1909). Geoscientific applications usually involve placing this cell in a furnace so that experiments can be carried out at different temperatures. In Knudsen-cell mass spectrometry, these gases are channeled directly to a mass spectrometer which allows one to identify the chemical and isotopic species that are effusing out. This presents a unique opportunity to carry out reactions within the cell and identify the fluids involved through continuous *in situ* monitoring of the gases that effuse out. The typical use of Knudsen cell mass spectrometry is in the field of equilibrium vapor pressure (and hence fugacity or activity) measurements, which allow thermodynamic mixing properties of solid and molten solutions to be calibrated (e.g., Rammensee and Fraser 1981). In our work we have made slight modifications to this conventional setup to specifically study mechanisms and kinetics of reactions involving crystalline material. Using a "crucible in crucible" setup, we are able to place the reactants (single crystals or powders) physically separated from each other such that they interact only via the mediation of a vapor phase (figure 1). A small amount of this vapor effuses out of the hole in the Knudsen cell, allowing a continuous, *in situ* sampling and monitoring of the vapor species present

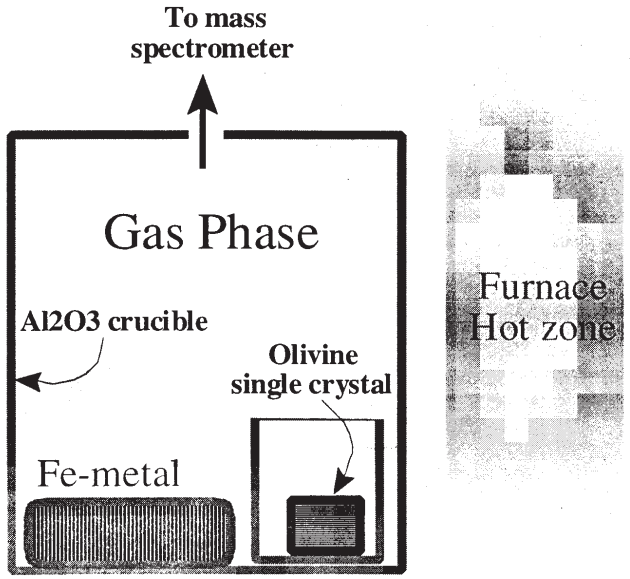

Figure 1. Schematic set up of Knudsen cell experiments to study kinetics of element exchange between two solid phases mediated by a vapor.

at each incremental time step during the reaction.

Analyses of the effusing vapor species can be carried out in real-time using a quadrupole mass spectrometer, which allows one to quickly scan across the masses relevant for the system under study. For example, for experiments in the system FeO-MgO-SiO_2, we were able to identify and semi-quantitatively analyze the concentrations of up to 4 species in the vapor phase (Fe, FeO, Mg and SiO), plus other species which may be present as background/contaminants (e.g., CO, CO_2), counting 2 seconds on each element and going through the full cycle every two minutes or so. For experiments lasting between 0.5–20 hours, this amounts to a continuous determination of the extent of reaction. Thus, we have data for the chemical composition of the reaction mediating fluid phase as well as how it evolves over time. These data, when combined with the composition of the solid phases which can be determined after the end of the experimental run using standard mineralogical analytical tools (e.g. optical microscopy, electron microprobe analyses, X-ray diffraction etc.), provides us with an unprecedented insight into the mechanisms by which chemical transformation takes place in minerals. Such studies have shown (e.g. Dohmen *et al* 1998, 2001) that even when transport rates are infinitely fast compared to all other processes (e.g., in an ideal gas), the low solubility of the species concerned in the fluid may lead to disequilibrium partitioning of elements at the crystal-fluid interface. As a concrete example, Dohmen *et al* measured fayalite contents in rims of olivine crystals coexisting, but not in contact, with metallic Fe. The mediat-

ing fluid in this case was a dry vapor phase—an ideal gas at high temperatures where mobility of species is high, but concentrations of Fe, Mg, Si and O bearing species are low. They found that

- the rim composition of olivine evolves with time i.e. equilibrium Fe-contents are not attained instantaneously relative to time scales of diffusion in the crystal and
- it is possible to obtain homogeneous fayalite rich crystals which are not in equilibrium with Fe—the composition of these crystals also evolve with time.

Such observations prompted us to consider the general case of the kinetics of element exchange mediated by a fluid phase, beacause this can have serious consequences for standard procedures in metamorphic petrology such as geothermometry and barometry.

1.2 *Transport or equilibrium properties?*

One of the standard assumptions implicit in most petrological interpretations of mineral chemistry and microstructure is that transport in the "intergranular fluid" is infinitely fast (Eiler *et al* 1992; Chakraborty *et al* 1997). In a few specific instances, this has been questioned recently for some metamorphic terranes (e.g. Florence and Spear 1995; O'Brien 1999 etc.). Concurrently, experimental studies of grain boundary diffusion rates have shown that while these are faster than volume diffusion rates through crystal lattices below some threshold temperature, the difference is only on the order of two orders of magnitudes (e.g. Farver *et al* 1994; Chakraborty *et al* 1994 etc.). On the other hand, diffusion coefficients in aqueous fluids are indeed found to be many orders of magnitude larger (up to 14 orders of magnitude!) than either of these (e.g. Watson and Wark 1997). This huge discrepancy in transport rates through dry grain boundaries vs. wet aqueous films in a polycrystalline matrix (i.e. rock) has focussed interest on the exact distribution of fluid phases and their connectivity through the consideration of dihedral angles (e.g. see Watson 1999 for a review). However, the efficiency of transport through such a grain boundary medium depends not only on transport rates, but also on the solubility of individual species in these fluids, as has been recognized in theoretical models (e.g. Mueller 1967; Fletcher and Hofmann 1974; Brady 1983) and demonstrated experimentally more recently by us, as noted above. Although some data are now available on the concentrations of major rock forming elements in various fluids, the implications of these solubilities for the chemical and mineralogical evolution of rocks have not yet been adequately explored. In this paper, we expand upon our recent work where we explored the consequences of coupling equilibrium thermodynamic parameters such as solubilities to transport models, and address the issue of how this affects the kinetics of element partitioning.

2. Theoretical model

2.1 *Model description*

In our model (figure 2), we consider the transfer, mediated by an intergranular fluid, of an element i between two initially homogeneous mineral grains, A and B, which are physically separated from each other. The mineral grains, taken to be rectangular slabs without loss of generality, are considered to be immersed in separate baths of the intergranular fluid. The two baths are connected to each other by a tube with a narrow aperture, representing a grain boundary. The model is analogous to the one used by Lasaga (1986) for his treatment of "kinetic isograds", although there are important differences between the two treatments. While our more comprehensive recent models have incorporated crystal growth or dissolution (e.g. Dohmen *et al* 2001), ignoring these complexities do not detract from the general applicability of the results in the present analysis as shown in Dohmen *et al* (2001). Instead, it is crucial for our purposes to account for the fact that minerals are solid solutions i.e., the proportions of different elements in a mineral grain can vary. This requires explicitly modelling compositional zoning due to volume diffusion within crystals—a feature not present in the treatment by Lasaga (1986). Our modelling involves splitting up the net exchange process into a series of steps leading to transfer of i from A to B (or vice versa) and applying the constraint of mass balance to each of these steps. It is assumed that i is the less soluble of the two species, i and j, involved in the exchange. Obviously, the total process involves a charge and lattice site compensating flux of species j in the reverse direction at each step. A and B can be two different minerals or two grains of the same mineral initially at different concentrations. The transfer, schematically illustrated in figure 2, is thought to proceed as follows:

(i) Concentration gradient within the crystal A drives a diffusion flux of i between the surface of the crystal and the interior volume according to Fick's first law of diffusion:

$$J_i^A = -D_A \cdot \left.\frac{\partial C_i^A}{\partial x}\right|_{x=\frac{LA}{2}} \tag{1}$$

where LA is the width of the crystal and the zero of the distance scale is placed symmetri-

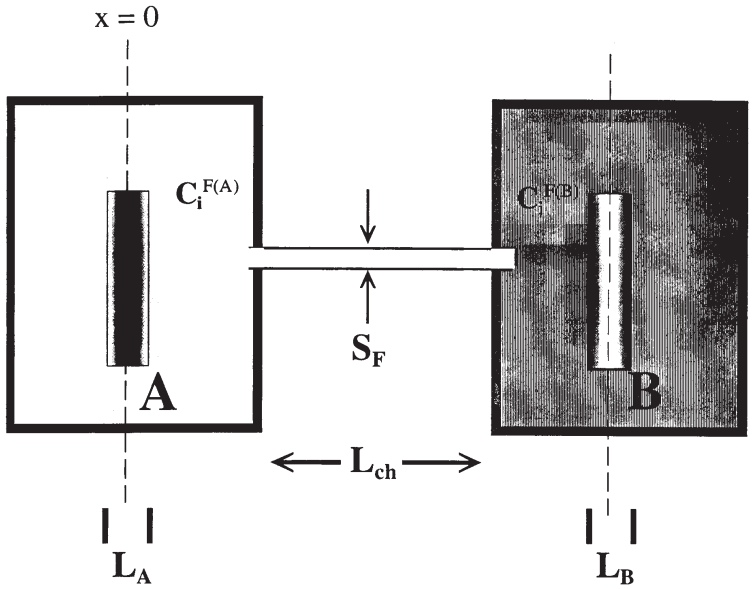

Figure 2. Schematic representation of model system showing element exchange between two zoned crystals, A and B, via an intergranular fluid present along a narrow tube (grain boundary). The crystals are considered to be immersed in their own bath of intergranular fluid. $C_i^{F(A)}$, $C_i^{F(B)}$ – concentration of i in the fluid surrounding A and B, respectively; L_A, L_B – width of the crystals A and B, respectively; S_F – cross sectional area of fluid channel.

cally along the middle of the crystal, J_i^A is the flux of i within the crystal volume of A, D_A and C_i^A are the diffusion coefficient and concentration, respectively, of i in A.

(ii) The number of atoms of i that are transferred from the fluid to the crystal (or the reverse) is considered to be proportional to the deviation from equilibrium. This deviation can be expressed in various forms—an operationally convenient one that we have chosen is the difference between the instantaneous concentration of i in the fluid bath surrounding A and the concentration that *would be* in equilibrium with the concentration of i at the surface of A at that point of time. This corresponds to surface reaction according to a linear rate law and differs from the arbitrary assumption of instantaneous equilibrium at the surface. The arbitrary assumption can lead to violations of mass or lattice site balance constraints so that some form of interfacial kinetic effect is required—the linear rate law represents the simplest form of kinetic hindrance and is consistent with our recent experimental results (Dohmen *et al* 2001). For the flux at the surface of A, we have:

$$J_i^{s(A)} = \alpha_A \cdot \left[C_i^{F(A)}(\text{Eq.}) - C_i^{F(A)} \right] = \alpha_A \cdot \left[K_{A/F} \cdot C_i^A \Big|_{\frac{L_A}{2}} - C_i^{F(A)} \right]_t . \quad (2)$$

Here, $J_i^{s(A)}$ is the flux of i across the surface of crystal A (into or from the fluid) at any given time $t, \forall_A$ is the kinetic constant for the linear rate law, $C_i^{F(A)}$ is the concentration of i in the fluid bath surrounding $A, C_i^{F(A)}$ (Eq.) is the concentration of i in the fluid bath that would be in equilibrium with the instantaneous concentration at the surface of A, and $K_{A/F}$ is the equilibrium partition coefficient, defined as concentration of i in the fluid divided by the concentration of i in crystal A (note that this is the reciprocal of the usual partition coefficients used in trace element geochemistry, where concentration in the mineral occurs in the numerator).

(iii) The atoms of i are transferred by diffusion along the "pipe" representing the grain boundary (filled with the "intergranular fluid") to the reservoir surrounding B. This process is assumed to proceed much faster than all other competing processes and at all points during the simulation a steady state distribution of the concentration of i is maintained in this intergranular region, given by

$$J_i^F = \frac{D_F}{L_{ch}} \cdot \left(C_i^{F(A)} - C_i^{F(B)} \right) \quad (3)$$

where J_F is the flux of i through the fluid, D_F is the diffusivity in the fluid (or any other appropriate transport coefficient, if transport in the fluid is not diffusion controlled.). L_{ch} is the length of the fluid channel and $C_i^{F(A)}$ and $C_i^{F(B)}$ are concentrations of i in the fluid baths surrounding crystals A and B, respectively.

(iv) Processes (ii) and (i) operate in reverse at B—an exchange of i takes place between the

reservoir surrounding B and the surface of B and the rate of this transfer is described by a linear rate law again. Following this, volume diffusion within B attempts to homogenize concentration gradients—the diffusion flux, of course, is proportional to the concentration gradient that is generated by exchange at the surface.

The partitioning of i between A and B is given by a partition coefficient, $K_{A/B}$, defined as (concentration of i in A)/(concentration of i in B) i.e., in a form appropriate for equilibrium constants in dilute solutions obeying Henry's Law. Considering the full exchange partition coefficient $\left(\frac{C_i^A}{C_i^B}\cdot\frac{C_j^B}{C_j^A}\right)$ merely introduces a time dependence of $K_{A/B}$, in the current problem, which makes the subsequent modelling numerically more complex, without introducing any qualitatively new behavior. Hence, we present our results using a constant, time-independent $K_{A/B}$ in this work. Further, without loss of generality and for the sake of simplicity, we have carried out all our simulations here for $K_{A/B} = K_{A/F}/K_{B/F} = 1$ i.e., at equilibrium, A and B have the same concentration (i.e., effectively stating that A and B are two grains of the same mineral which have different compositions initially, although later on we attribute different diffusion rates of i to A and B). We would like to emphasize however, that it would have been inconsequential in terms of observation of the qualitative range of behavior had we chosen any other value or functional form for $K_{A/B}$, but this choice makes the graphical illustrations that follow more direct.

2.2 *The equations and the boundary conditions*

The basic equations are obtained by imposing mass balance constraints on each kind of flux at each junction. The flux of i into (or out of) the surface of A must equal the diffusive flux to (or from) the interior of A due to volume diffusion, i.e., we equate fluxes from equations (1) and (2) for A

$$-D_A\cdot\left.\frac{\partial C_i^A}{\partial x}\right|_{x=\frac{LA}{2}} = \alpha_A\cdot\left[K_{A/F}\cdot C_A\big|_{\frac{LA}{2},t} - C_i^{F(A)}\right]. \quad (4)$$

The above equality applies when expressions on either side in equation (4) are integrated over the entire surface of the crystal—but since the same surface area term, that of crystal A, appears on both sides, these cancel out.

Next, we equate fluxes from equations (2) and (3) at the left to state that the flux of i out of (or into) the surface of A integrated over the entire surface area, must be balanced by net, integrated flux into (or out of) the fluid i.e.,

$$\alpha_A\cdot S_A\cdot\left[K_{A/F}\cdot C_i^A\big|_{\frac{LA}{2},t} - C_i^{F(A)}\right] = \frac{S_F\cdot D_F}{L_{ch}}\cdot\left(C_i^{F(A)} - C_i^{F(B)}\right). \quad (5)$$

Here, S_F is the cross-sectional surface area of the fluid conduit and S_A is the total surface area of grain A, i.e., in contrast to equation (4), the surface terms on the two sides of the equation are different here and the ratio (rather than absolute values of the surface areas) S_F/S_A, roughly related to the porosity of the rock (assuming all pore space is filled with fluid), plays an important role, as we will find in the simulations that follow. The parameters S_F and L_{ch} together effectively characterize the permeability of this system.

Similarly, we obtain two equivalent equations for the right hand side of the system i.e., for B. Expressing the diffusion flux expression in equation (4) and its equivalent for B in their finite difference forms, we have a set of 4 linear algebraic equations with the 4 unknowns, $C_i^{F(A)}$, $C_i^{F(B)}$, $C_i^A[LA/2,t]$ and $C_i^B[LB/2,t]$. Thus we can explicitly solve for the values of the unknown parameters. Having obtained the concentrations at the rims of the crystals, $C_i^A[LA/2,t]$ and $C_i^B[LB/2,t]$ at any given time t, the corresponding concentration profile within the crystal may then be calculated numerically using a finite difference scheme. An additional boundary condition is obtained by imposing in each case the additional constraint due to symmetry, e.g., $J_i^A = 0$ at the center of the crystal. The relevant parameters which describe the system are:

D_A	$\equiv$	the diffusion coefficient of i in A.
D_B	$\equiv$	the diffusion coefficient of i in B.
D_F	$\equiv$	the diffusion coefficient of i in the fluid.
L_{ch}	$\equiv$	the length of the fluid channel.
S_F	$\equiv$	the cross-sectional surface area of the fluid channel. In combination with L, this is related to porosity in a natural system
S_A, S_B	$\equiv$	surface area of crystals A and B, respectively.
L_A, L_B	$\equiv$	width of crystals A and B, respectively.
$\forall_A$	$\equiv$	the linear rate law kinetic constant for A.
$\forall_B$	$\equiv$	the linear rate law kinetic constant for B.
$K_{A/F}$	$\equiv$	the partition coefficient of i between fluid and mineral A.
$K_{B/F}$	$\equiv$	the partition coefficient of i between fluid and mineral B.

For the following simulations, we have fixed the values of some of these parameters and explored the effect of the others. Mean values of parameters, around which we have explored the variations, are as follows: $K_{A/F} = K_{B/F}$ (as discussed above) $= 10^{-7}$, which is reasonable considering the thermodynamic data for aqueous species (e.g., Oelkers *et al* 1995) and solid phases (e.g., Berman 1988) for elements like Fe and Mg at temperatures of about 700–800°C, which are of interest here. The diffusion rates in the solids were fixed at $10^{-20}\,m^2/sec$, consistent with experimentally determined diffusion rates of Fe and Mg in minerals like garnets at 800°C (e.g., Ganguly *et al* 1998). Diffusion rates in the fluid were set to a much larger value of $10^{-7}\,m^2/sec$, consistent with the results obtained by Watson and Wark (1997) for silica diffusion in water. The grain size of the crystals were taken to be 1 mm and the fluid to solid surface area ratio, (S_F/S_A) and (S_F/S_B), were set equal to each other at 10^{-3}. This is an approximation for porosity in this model system. Finally, the kinetic constants $\forall$ were set to their ideal value, unity, in the absence of any available experimental data. We note however that there are indications that these constants may have values on the order of 10^{-3} (e.g., see Dohmen *et al* 2001), in which case all the inferred disequilibrium effects will be substantially magnified, as is illustrated below.

3. Results and discussion

Although our model incorporates a parameter describing the surface reaction kinetics ($\forall_A$ and $\forall_B$), we have not explored the hindrance caused specifically by these in the present work except in one case. Most of our interesting kinetic results come from considering the effects of the concentration of the element of interest in the intergranular fluid which would be in equilibrium with the crystals, which emphasizes the coupling between thermodynamics and kinetics. Also, note that the absolute values of the surface areas of mineral A and B, parameters which are somewhat difficult to determine, are inconsequential—it is the ratios (S_F/S_A) and (S_F/S_B) that play an important role in the compositional evolution of the system.

We have adopted the following scheme (figure 3) to illustrate our results. In the symmetric systems that we have modelled (grain size and surface area of A and B are the same in each simulation), normalized concentration plots show crystals A and B at equilibrium when the concentrations are homogeneous at 0.5 (this is the consequence of choosing $K_{A/B} = 1$). The concentrations in the fluid are of course much lower (by factors of about 10^{-7}). In order to illustrate these on the same scale, concentrations in the fluid are divided by the equilibrium partition coefficient $K_{A/F}$ $(= K_{B/F}$, in all cases studied here) such that at equilibrium, the compositions at the rim of the crystal and in the fluid will be the same on these normalized plots. At overall equilibrium, we would obtain a flat, homogeneous *normalized concentration* distribution across both crystals and the fluid, which levels off at a value of 0.5 on the normalized concentration axis.

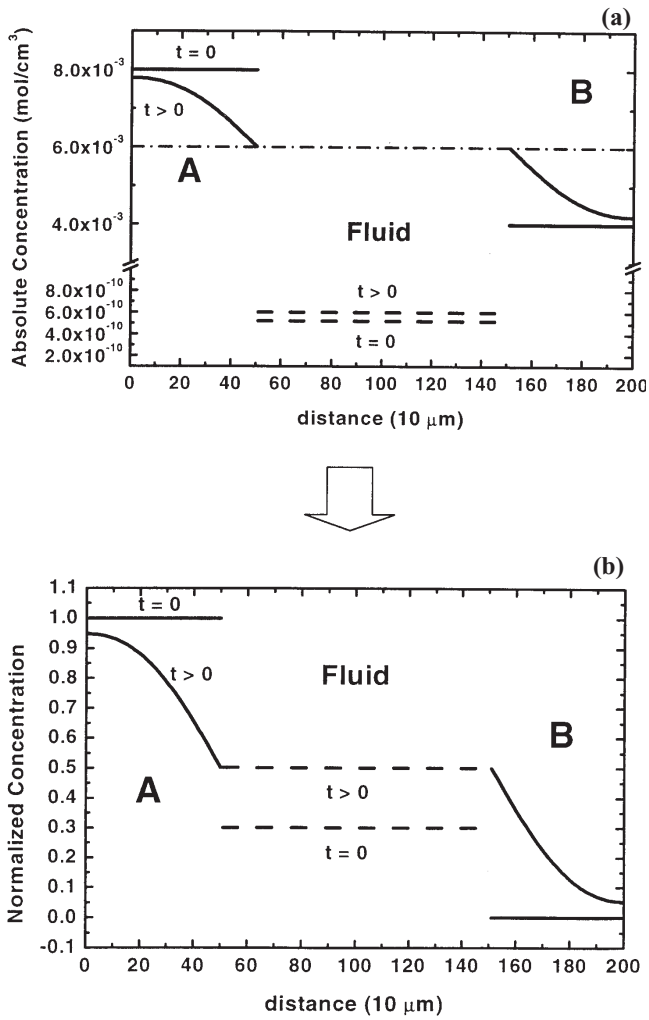

Figure 3. Schematic illustration of the model and the normalization scheme. **(a)** Absolute concentration (moles/cm^3) plotted as a function of distance in mineral A, fluid and mineral B. Initially, at time $t = 0$, concentration distribution is homogeneous in all three phases. At a later time $t > 0$, minerals A and B are zoned, and the fluid is either homogeneous or has a concentration gradient that is not discernible on this scale. **(b)** The same plot, using the normalization scheme outlined in the paper. Now, initially, mineral A has a concentration of 1.0, mineral B has 0.0 and the fluid (after division by the partition coefficient, see text) is at 0.3. At later times, $t > 0$, the minerals are zoned and the fluid is illustrated as homogeneous. At equilibrium, all three phases will attain a value of 0.5 on such a plot (as long as the grain sizes of A and B remain the same).

Using this scheme, figure 4 (a–f) show some results of simulations and table 1 gives the values

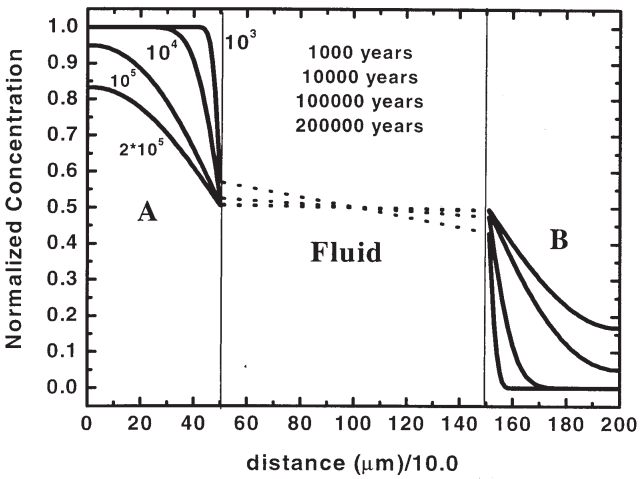

Figure 4(a). Model simulations showing concentration distribution as a function of distance in the two crystals as well as the fluid. The concentration axis is normalized, such that initial concentration in crystal $A = 1.0$, in $B = 0.0$. The concentration in the fluid is too low to be shown on the same scale, so it is scaled up by a factor equivalent to the partition coefficient, such that at equilibrium, the fluid composition as represented here will have the same value as the adjacent solid. Equilibrium in these symmetric systems with $K_{A/B} = 1$ (and same grain size and surface area of the two solids) is attained when concentration in $A = B =$ Fluid, as shown here $= 0.5$. **(a)** Concentration evolution as a function of time in an evolving system. The labels on curves denote time in years.

of the parameters used to obtain these. The attainment of steady state in the fluid has been verified through detailed calculations where the diffusion in the fluid was modelled explicitly. It is found that after only a few timesteps (exact number depending on the magnitudes of D_A and D_B) a steady state is attained in the fluid, thereby justifying our formulation of equation (3). However, the attainment of steady state does not necessarily imply that the surfaces of A and B are in equilibrium with the fluids in the vicinity of A and B, $C_i^{F(A)}$ and $C_i^{F(B)}$, respectively. Alternately, the surfaces of the minerals may be in equilibrium with the fluid in their vicinity but not with each other—not as a consequence of slow transport rates in the fluid but because of low concentration of i in the fluid. With further evolution, both crystals become compositionally zoned, where the extent of zoning in each mineral depends on the diffusion coefficient of i in that mineral. This sequence of events is illustrated in figure 4(a), where, for the above choice of parameters, it is found that within the first 1000 years, the surfaces of the crystals are in equilibrium with the adjacent fluid but not with each other. The crystals are essentially unzoned at this stage. After 10,000 years, the crystals have attained equilibrium with the fluid and with each other at their rims, and a substantial concentration gradient has developed within the crystals due to diffusion. With subsequent progress of time, by 100000 years, the crystal is zoned all the way to its core and with continued diffusion it eventually progresses to homogenization and overall equilibrium. This is the general state of affairs that is usually assumed to have taken place during the evolution of a rock—the simulation merely demonstrates that the current model is realistic in that sense. In the subsequent simulation runs, we explore the role of various parameters and how they may lead to unexpected behavior in some cases, even for small variations.

Figure 4(b) illustrates the effect of varying the concentration of i in the intergranular fluid. Such variations may be obtained even at constant P, T and bulk chemistry through variations in parameters such as oxygen fugacity and pH. It is found that up to a threshold value of solubility of 10^{-8}, the behavior is straightforward—equilibrium at the surface in contact with the fluid, diffusion zoning within the crystal. However, in spite of the rapid transport rate in the fluid with further drop in $K_{A/F}$ and $K_{B/F}$, the compositions at the surfaces of the crystals are in equilibrium with the fluid but not with each other anymore, and within a couple of orders of magnitudes, by 10^{-11}, the system is completely frozen so that the crystals remain fixed at their initial compositions i.e., the intergranular fluid has become an ineffective trans-

Table 1. *Table showing the parameter sets used for the various simulations. The parameters, whose roles are specifically explored in a given simulation, are shown in bold.*

Figure	D_F (m^2/s)	D_A (m^2/s)	D_B (m^2/s)	K_A	K_B	S_F/S_A	S_F/S_B	$\forall_A$ (m/s)	$\forall_B$ (m/s)
3a	10^{-7}	10^{-20}	10^{-20}	10^{-8}	10^{-8}	10^{-3}	10^{-3}	1	1
3b	10^{-7}	10^{-20}	10^{-20}	**variable**	**variable**	10^{-3}	10^{-3}	1	1
3c	10^{-7}	10^{-20}	10^{-20}	10^{-8}	10^{-8}	**variable**	**variable**	1	1
3d	10^{-7}	10^{-18}	10^{-20}	**variable**	**variable**	10^{-3}	10^{-3}	1	1
3e	10^{-7}	10^{-18}	10^{-20}	10^{-8}	10^{-8}	10^{-3}	10^{-3}	10^{-5}	**variable**
3f	10^{-7}	10^{-20}	10^{-20}	10^{-7}	10^{-7}	10^{-3}	10^{-3}	1	1

Note: For simulations in figure 4(b–e), the concentration distributions are shown after 100,000 years.

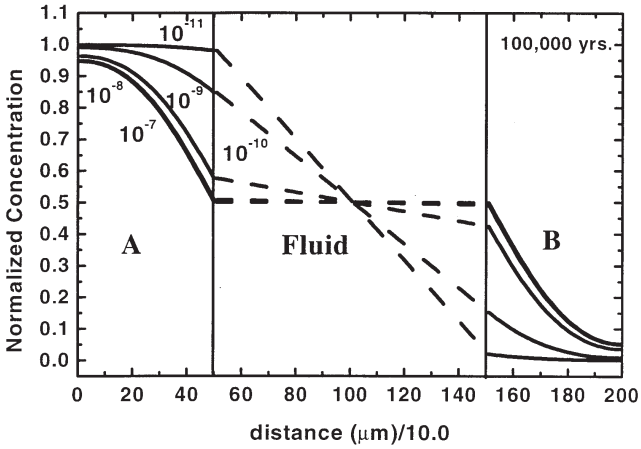

Figure 4(b). The effect of partition coefficient between fluid and solid on the evolution of the system, illustrated 100,000 years after start of reaction. The curves are labelled with values of $K_{A/F}$. Note that in this system, for $K_{A/F} > 10^{-8}$, there is no influence of this parameter on the kinetics; for $K_{A/F} < 10^{-11}$, the system is frozen.

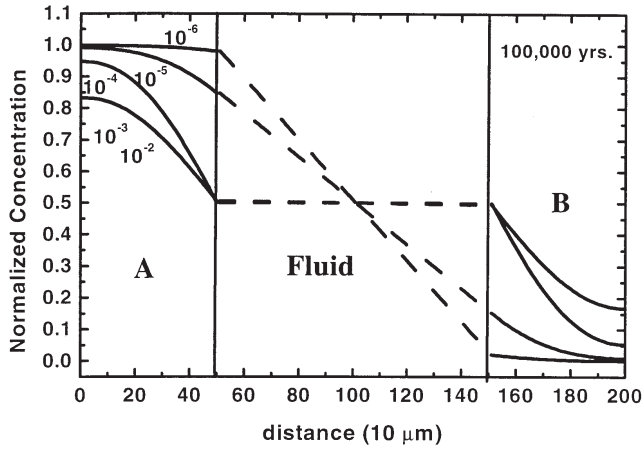

Figure 4(c). The effect of surface area/porosity on the evolution of the system, illustrated 100,000 years after start of reaction. The curves are labelled with values of the parameter S_F/S_A. Again, note that there is a window in the range of this parameter where it affects the kinetics—above 10^{-3} the parameter has no influence and below 10^{-6}, the system is frozen.

port agent. This behavior has been observed experimentally in experiments designed to study the effect of water on cation diffusion rates in garnets (J Ganguly, pers. comm.). The exact value of the threshold limit of solubility (e.g., 10^{-8} in this case) depends on factors like porosity and permeability (i.e., S_F/S_A, S_F/S_B and L_{ch} in our model) and the kinetic constants ($\forall$). Indeed, varying these parameters at constant $K_{A/F}$ and $K_{B/F}$ has a very similar effect, as illustrated in figure 4(c). Here ($K_{A/F} = K_{B/F} = 10^{-8}$, corresponding to surface equilibrium in figure 4b), equilibrium is obtained at the surface of the crystals for values of (S_F/S_A) and (S_F/S_B) up to 10^{-4}. As these ratios drop below this value, although equilibrium is still obtained at the surface, the extent of compositional zoning within the crystal is different. This emphasizes the perils of interpreting compositional zoning within crystals without paying proper attention to the boundary conditions. With further drop in these ratios, the surfaces of the two minerals fail to reach equilibrium with each other and ultimately the system freezes, as above for low values of $K_{A/F}$ and $K_{B/F}$, by the time S_F/S_A and S_F/S_B reach 10^{-6}. Again, the specific threshold values are obtained for the given choice of parameters here and can be changed by altering the solubilities, $K_{A/F}$, for example. This emphasizes yet another important point—different trace elements in the same system may show different classes of behavior! And of course, the simplifying assumption that we have made by assuming $S_A = S_B$ need not hold in any natural system and one may obtain different classes of behavior for different minerals, or even the same mineral present in different grain sizes!

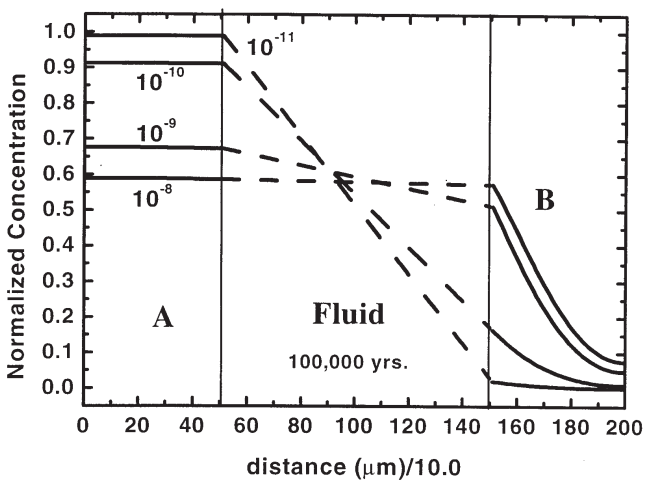

Figure 4(d). The effect of different diffusion rates in solids combined with differences in partition coefficients. Diffusion coefficient in A taken to be 10^{-18}, in B 10^{-20}. The curves are labelled by the values of $K_{A/F}$. Note that mineral A, with the faster diffusion coefficient, homogenizes while mineral B stays zoned. However, the rim compositions of A and B are not necessarily in equilibrium with each other, although they are both in equilibrium with the adjacent fluid.

The cases considered so far deal with minerals that are similar in their diffusion behavior e.g., garnets and pyroxenes as they occur in mantle xenoliths or granulite facies metamorphic rocks. In figure 4(d) we explore the situation where the diffusion rate in one of the minerals of the exchange couple is much faster, as is the case for example, when garnet and biotite exchange Fe-Mg. Here, we have increased D_A to $10^{-18}\,\mathrm{m}^2/\mathrm{sec}$ i.e., two orders of magnitude faster diffusion than in B. The result is as anticipated from intuition and observations in natural systems—A remains unzoned while

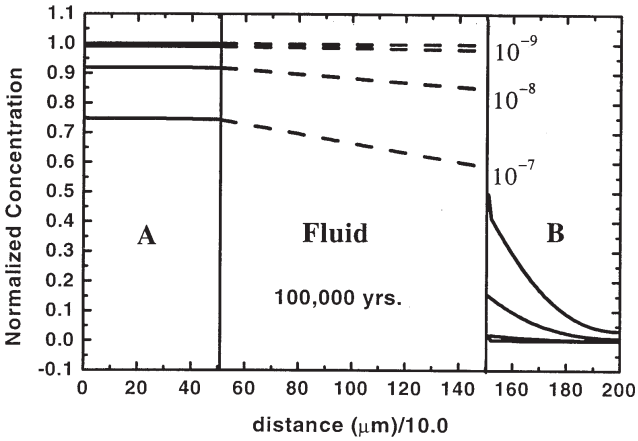

Figure 4(e). The effect of the kinetic rate constant, $\forall$ leading to pure interface controlled reaction.. The curves (after 100,000 years in each case) are labelled by the different values of α_B. Diffusion coefficient in A was taken to be faster ($10^{-18}\,\mathrm{cm}^2/\mathrm{s}$) than in B ($10^{-20}\,\mathrm{cm}^2/\mathrm{s}$). α was varied only for the mineral B, with α_A held constant at 10^{-5}. Note that in this case, for values of $\alpha_B < 10^{-7}$, the surface of B is no more in equilibrium with the adjacent fluid and the composition of the fluid is buffered by the composition of A.

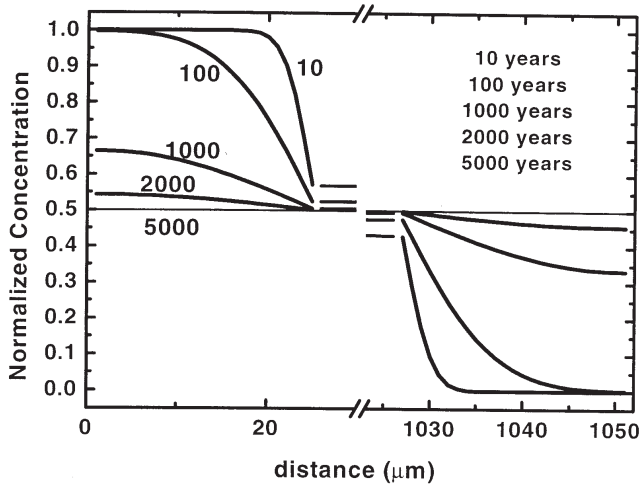

Figure 4(f). The effect of grain size. The parameters for this plot are the same as in figure 4(a), excepting that the grain sizes of the crystals have been reduced to 50 microns (compared to 1000 microns in (a)–(e)). The time evolution of composition is shown and the curves are labelled with values of time in years. Note difference in time scale between this plot and (a).

B is zoned. However, the interesting behavior is obtained by now varying the concentration in the intergranular fluid, $K_{A/F.}$. We have already seen in figure 4(b) that for $K_{A/F} = 10^{-8}$, the fluid is in equilibrium with the surfaces of A and B. Once the diffusion rate in A is increased, the entire crystal is in equilibrium, as seen in figure 4(d). However, when the solubility drops now, unlike figure 4(b), we have a homogeneous crystal of A in each case, in equilibrium with the adjacent fluid, but out of equilibrium even with the rim composition of B, with which it is constantly communicating via a fluid in which transport rate is fast! This is a reasonable but counter intuitive result, which tells us that the presence of a fluid in which diffusion rates are fast (e.g., an aqueous fluid) does not guarantee equilibrium between the rim of a crystal and other homogeneous crystals at different distances from it. Clearly, use of such mineral pairs for geothermometry or barometry will yield results devoid of any physical significance.

Finally, we want to explore the effect of varying the kinetic constant, $\forall$. Values of $\forall$ are practically unknown in mineralogical systems and modelling studies such as this indicate the need to measure these quantities experimentally. However, the consequence of variation in this quantity can be seen in figure 4(e). Here, we have maintained the faster diffusion rate in A such that A always remains homogeneous. $\forall_A$ was fixed at 10^{-5} and $\forall_B$ was varied from 10^{-5} downwards. It is found that for $\forall_B < 10^{-7}$, the surface of B is not anymore in equilibrium with the adjacent fluid and we have the case of true interface controlled reaction, where the fluid composition is buffered by the composition of A.

As a last example, we explore the effect of grain size—we return to the original parameter space of figure 4(f), and simply reduce the grain sizes of both A and B to 25 microns from 1 mm. We find that surface equilibrium is attained within 100 years, and the crystals are practically homogeneous in 5000 years. This merely confirms the anticipated drastic role of grain sizes. If we assume A to have a large surface area and/or faster kinetics (surface reaction as well as volume diffusion rate), then the concentration of i in the fluid is effectively buffered by A very soon after reaction starts. The problem then reduces to tracking the evolution of B as a function of time. This situation may arise, for instance, when A is extremely fine grained.

The significant observation in all of the above is that the concentrations at the rims of both crystals are not in equilibrium with each other even though a steady state gradient develops in the fluid rapidly because of the fast transport rates in the fluid. The slower reaction times of the solids imply that this gradient is maintained in the fluid i.e., such an intergranular fluid is not homogeneous! The disequilibrium between different grains is primarily a consequence of the low solubility of i in the fluid, which does not allow A and B to communicate with each other efficiently, as opposed to fast, enough. Very similar effects are therefore obtained when the permeabil-

ity of the system is reduced instead of the solubility.

It is found that a drop in permeability by about a couple of orders of magnitude below a certain threshold "freezes" the system, the minerals hardly evolve from their initial concentrations. In this case we have two homogeneous minerals, which have, however, never been in equilibrium with each other! Conversely, this is a good illustration of how brittle deformation, in particular in conjunction with chemical reactions involving relatively large volume changes (e.g., dehydration) may open up cracks, thereby enhancing permeability and in turn, reaction rates—an observation made frequently in metamorphic rocks (e.g., Rubie 1986; Jamtveit *et al* 1990; Dempster and Tanner 1997). Influx of fluid (such as those released by dehydration) through such cracks, can of course contribute further to this enhancement.

4. Conclusion

A rich variety of behavior can be obtained, in models and by inference in nature, through various combinations of the relevant parameters discussed above—only a small range of the entire parameter space has been explored here. However, these illustrations should serve to underscore the importance of understanding, or at least having a feel for, actual reaction mechanisms before applying conventional tools like thermometers and barometers to mineral assemblages—clearly, some of the "time tested" criteria e.g., homogeneity of minerals and use of rim compositions of minerals as "proofs" of equilibrium can be very fallible. Similarly, interpretations of closure temperatures and dates obtained from mineral chronometry are not exempt from the above considerations. The situation may, however, be turned to our advantage—modelling concentration distributions in natural rocks using tools such as these may actually provide direct information about the nature of the elusive "intergranular fluid"—finally.

Acknowledgements

Critical comments by Profs. R Kretz and J Ganguly helped us to significantly improve the clarity of presentation. The research presented here has been supported by funds from the German Science Foundation (DFG).

References

Berman R G 1988 Internally consistent thermodynamic data for minerals in the system Na_2O-K_2O-CaO-MgO-FeO-Fe_2O_3-Al_2O_3-SiO_2-TiO_2-H_2O-CO_2; *J. Petrol.* **29** 445–522

Brady J B 1983 Intergranular diffusion in metamorphic rocks; *Am. J. Sci.* **283** 181–200

Chakraborty S, Lasaga A C and Bolton E W 1997 Diffusion controlled fractionation of trace elements in magmatic systems. AGU Fall Meeting; *EOS* **78** F833

Chakraborty S, Farver J R, Yund R A and Rubie D C 1994 Mg tracer diffusion in synthetic forsterite and San Carlos Olivine as a function of P,T and fO_2; *Phys. Chem. Min.* **21** 489–500

Dempster T J and Tanner P W G 1997 The biotite isograd, Central Pyrenees: a deformation-controlled reaction; *J. Metamorphic Geol.* **15** 531–548

Dohmen R, Chakraborty S, Palme H and Rammensee W 2001 The role of element solubility on the kinetics of element partitioning: *in situ* observations and a thermodynamic kinetic model; *J. Geophys. Res.*, in review.

Dohmen R, Chakraborty S, Palme H and Rammensee W 1998 Solid-solid reactions mediated by a gas phase: An experimental study of reaction progress and the role of surfaces in the system Olivine + Fe-metal; *Am. Min.* **83** 970–984

Eiler J M , Baumgartner L P and Valley J W 1992 Intercrystalline stable isotope diffusion: a fast grain boundary model; *Contrib. Mineral. Petrol.* **112** 543–557

Farver J R, Yund R A and Rubie D C 1994 Magnesium grain boundary diffusion in forsterite aggregates at 1000°C – 1300°C and 0.1 MPa to 10 GPa; *J. Geophys. Res.* **99** 19809–19819

Fletcher R C and Hofmann A W 1974 Simple models of diffusion and combined diffusion-infiltration metasomatism; In *Geochemical Transport and Kinetics* (eds) A W Hofmann, B J Giletti, H S Yoder Jr, and R A Yund, (D C Washington, Carnegie Inst. Washington) p. 243–259

Florence F P and Spear F S 1995 Intergranular diffusion kinetics of Fe and Mg during retrograde metamorphism of a pelitic gneiss from the Adirondack Mountains; *Earth and Planet. Sci. Lett.* **134** 329–340

Ganguly J, Cheng W and Chakraborty S 1998 Cation diffusion in aluminosilicate garnets: experimental determination in pyrope almandine diffusion couples; *Contrib. Mineral. Petrol.* **131** 171–180

Jamtveit B, Bucher-Nurminen K and Austrheim H 1990 Fluid controlled eclogitization of granulites in deep crustal shear zones, Bergen Arcs, Western Norway; *Contrib Mineral. Petrol.* **104** 184–193

Knudsen M 1909 Die Molekularströmung der gase durch Öffnungen und die Effusion; *Ann. Phys.* **28** 999–1016

Lasaga A C 1986 Metamorphic reaction rate laws and development of isograds; *Min. Mag.* **50** 359–373

Mueller R F 1967 Mobility of the elements in metamorphism; *J. Geol.* **75** 565–582

O'Brien P J 1999 Asymmetric zoning profiles in garnet from HP-HT granulite and implications for volume and grain-boundary diffusion; *Min. Mag.* **63** 227–238

Oelkers E H, Helgesson H C, Shock E L, Sverjensky D A, Johnson J W and Pokrovskii V A 1995 Summary of the apparent standard partial molal Gibbs Free Energies of formation of aqueous species, minerals, and gases at pressures 1 to 5000 bars and temperatures 25 to 1000°C; *J. Phys. Chem. Ref. Data* **24** 1401–1553

Rammensee W and Fraser D 1981 Activities in solid and liquid Fe-Ni and Fe-Co alloys determined by Knudsen cell

mass spectrometry; *Ber. Bunsen. Phys. Chem.* **85** 588–592

Rubie D C 1986 The catalysis of mineral reactions by water and restrictions on the presence of aqueous fluid during metamorphism; *Min. Mag.* **50** 399–415

Watson E B 1999 Lithologic partitioning of fluids and melts; *Am. Min.* **84** 1693–1710

Watson E B and Wark D A 1997 Diffusion of dissolved SiO_2 in H_2O at 1 GPa, with implications for mass transport in the crust and upper mantle. *Contrib. Mineral. Petrol.* **130** 66–80